BUDAPEST UNIVERSITY OF TECHNOLOGY AND ECONOMICS
FACULTY OF MECHANICAL ENGINEERING
GÉZA PATTANTYÚS-ÁBRAHÁM DOCTORAL SCHOOL OF MECHANICAL ENGINEERING SCIENCES

The role of nitrogen in duplex stainless steel welding

Theses

Author:

Balázs Varbai
mechanical engineer
european welding engineer (EWE)
international welding engineer (IWE)

Supervisor:
Dr. habil. Kornél Májlinger
associate professor

Budapest, 2019

The critiques of the dissertation and the minutes of the defense can later be found in the Dean's Office of the Faculty of Mechanical Engineering of Budapest University of Technology and Economics

INTRODUCTION AND PROBLEM STATEMENT

Stainless steels according to the Hungarian and European standard MSZ EN 10088:2015 are those steels which have a chromium content of at least 10.5 % and a carbon content of up to 1.2 %.

According to the 2018 report by the International Stainless Steel Forum (ISSF) [1], the worldwide production of stainless steels reached 45.4 million tonnes by the end of 2018 [2]. Stainless steels are divided into three groups according to their application: (i) corrosion-resistant steels, (ii) heat-resistant steels and (iii) creep-resistant steels. Also, according to MSZ EN 10088-1, types of stainless steels are classified into four subgroups based on their microstructure: (i) austenitic, (ii) austenitic-ferritic (duplex), (iii) ferritic, and (iv) martensitic, and precipitation hardening types.

Duplex stainless steels contain more nickel as an alloy element than ferritic types, but typically less than the austenitic ones (Ni = 1-9 %). According to their chemical composition, duplex stainless steels can be divided into four main groups: (i) lean duplex steels with reduced Ni and Mo, (ii) Cr = 22 %, Ni = 5 %, Mo = 3 % and N = 0.20 % standard duplex steels, (iii) super-duplex steels with increased Cr and W content; (iv) hyperduplex steels with increased Cr and Mo content.

The industrial application of duplex stainless steels has been steadily increasing since the 1990s [3, 4], but in terms of the total stainless steel use, the usage of duplex steels are barely 1% [5, 6]. However, this 1 % usage means 18 % of stainless steel failure in the oil and gas industry [6].

In duplex steels, the ideally equal austenitic-ferritic microstructure combines the advantages of austenitic and ferritic corrosion-resistant steels, i.e. high strength and corrosion resistance [7, 8]. The ideal phase ratio formed in the duplex base metal is due to the presence of austenite- and ferrite-promoting alloys in the appropriate amount and the result of a well-chosen thermal cycle.

In addition to the classical alloys of stainless steels (Cr, Ni, Mo), duplex steels are alloyed to a high degree with nitrogen (N> 0.19 %). N-alloying strongly improves resistance to pitting corrosion and increases yield strength ($R_{p0.2}$ = 500 MPa). Nitrogen is also an austenitic promoter, interstitial element that is of particular importance when welding duplex steels.

For welding duplex steels in industry is tungsten electrode (TIG) welding is widely applied. Generally speaking, the use of appropriate filler material and / or nitrogen-containing (argon-based) shielding gas is essential for TIG welding of duplex steels. The diatomic N_2 in the argon shielding gas mixture dissociates in the arc plasma to atomic nitrogen (*N*), which dissolves in the molten pool

[9]. The dissolved *N* in the weld metal can exert its austenite-forming function as a function of the cooling time (heat input). In case of low heat input welding processes (such as laser beam welding), the weld metal and the heat affected zone remains almost completely ferritic [10, 11], which can lead to a reduction in toughness and Cr_2N precipitation. In the case of higher heat input process the longer cooling time allows *N* to exert its austenitic-forming, strength and corrosion resistance enhancing effect. However, the relationship between the N_2 content of the shielding gas, the dissolved *N* content of the weld metal and the austenite content is not always comprehended.

Başyiğit et al. [12] used various N_2-containing shielding gases for TIG welding of duplex steel 2205. According to their measurements, the average austenitic content of the weld metal decreased by 1.4 % when using a shielding gas containing 3 % N_2, compared to welding with 1 % N_2 shielding gas. With shielding gases containing 6 % and 9 % N_2, the austenite content of the weld metal has increased to over 60 %. Higher N_2-containing shielding gas (up to 20 % N_2) was used by Westin et al. According to their measurements, the austenite content of the weld metal was reduced by ~2 % when using a shielding gas containing 10 % N_2 compared to welding with a shielding gas of 5 % N_2. Pamuk et al. [14] used N_2-containing shielding gas for TIG welding of 2205 duplex steel. The austenite content of the root side was reduced in the case of gas protection containing 10 % and 15 % N_2 compared to the result of welding with Ar + 5 % N_2 gas shielding gas. In order to demonstrate the contradictory effects of N_2 mixed argon shielding gases the following representation is collected for the case of TIG welding of different duplex materials, using Ar + 5 % N_2 shielding gas.

Westin [13] has found that, the austenite content increased to 62 % in the weld metal, using shielding gas containing 5% N_2. Igual Muñoz et al. [15] measured 82 % austenite content in the weld metal by TIG welding of 2205 base materials with 5 % N_2 gas shielding. Migiakis et al. [16] measured 73-83 % austenitic content in the weld metal, depending on the type of filler materials, when welding UNS S32760 duplex steel. Reyes-Hernández et al. [17] measured 73 % austenite content in the weld metal with using 5 % N_2 gas protection for 2205 duplex steel welding. Bhatt et al. [18] measured 65 % austenite content in the weld metal of U-50 (~ 22Cr-7Ni-3Mo) duplex stainless steel, using 5 % N_2 gas protection.

Summarizing the effects of the nitrogen as a shielding gas, it can be said that its austenite-promoting effect is hihgly depends on the interaction of complex processes of arc welding.

OBJECTIVES

In order to clarify the effects of argon mixed nitrogen shielding gas, I deconstructed the complex arc welding process into its elements and investigated the effects of each element on the formed austenite content, individually. The evaluation of each process is based on the austenite-forming effect of nitrogen (N) initially dissolved in the base material and the diatomic nitrogen (N_2) mixed in the shielding gas during TIG welding.

- My goal was to show the qualitative and quantitative effects of initially dissolved *N* in the base material and N_2 mixed to the shielding gas on the austenite and nitrogen content of the heat affected zone and the weld metal.
- I aimed to investigate the effect of the dissolved *N* and the cooling time associated with arc energy, on the austenitic content of heat affected zone.
- In the case of weld metal, my goal was to determine the amount of nitrogen reduction as a function of arc energy in TIG welding, using Ar shielding gas and no filler metal.
- My aim was also to develop a model for determining the effect of N_2 mixed with shielding gas on the total dissolved *N* content of the weld metal as a function of heat input.

THE USED BASE MATERIALS AND THE STRUCTURE OF THE RESEARCH WORK

For the welding experiments the industrially most widely used standard duplex stainless steel X2CrNiMoN22-5-3 (2205) and two new types of lean duplex stainless steel X2CrMnNiN21-5-1 (2101) and X2CrNiMnMoCuN24-4-3-2 were chosen. The structure of the research work is as follows.

In order to determine the austenite content, it is essential to develop a suitable method to measure the austenite content of the base material, the heat affected zone and the weld metal, based on metallographic examination. For the austenite content measurement with image analysis software, I determined an optimum etching cycle using Beraha-II (85 mL HCl + 15 mL H_2O + 1 g $K_2S_2O_5$) etchant.

In order to investigate the effect of *N* dissolved in the base material and the effect of cooling time on the austenite content of the heat affect zone, samples were made with Gleeble thermomechanical simulator and TIG weld-

ing without filler material (142). Based on the results, I have established a relationship that can be used to determine the amount of austenite phase formed in the heat affected zone as a function of cooling time.

During the investigation of the weld metal, I made welded samples, using different N_2-containing (0-50%) Ar-based shielding gases, with the welding procedure of 142. Based on the results I have constructed a model to determine the dissolved nitrogen content of the weld metal after solidification.

As a next step, the total dissolved *N* content and austenite content of the weld metal of autogenous TIG welded samples with Ar shielding gas were investigated as a function of arc energy. The purpose was to determine the relationship between the nitrogen reduction in the weld metal and the applied arc energy.

RESULTS OF THE RESEARCH WORK

Determination of austenite content by metallographic method

Fort he determination of austenite content, the image analysis method can be used, however special care should be taken ont he contrast level between the ferritic and austenitic phases while applying chemical etching with Beraha-II etchant.

I have determined the etching cycles for all the investigated material grades, which gives the highest contrast between the austenite and ferrite phases. Tthe austenite content was measured by image analysis software on these samples. The value of the austenite content thus obtained was validated by ferritescope (see Figure 1), backscattered electron diffraction, and manual point count (according to ASTM E562-1) methods.

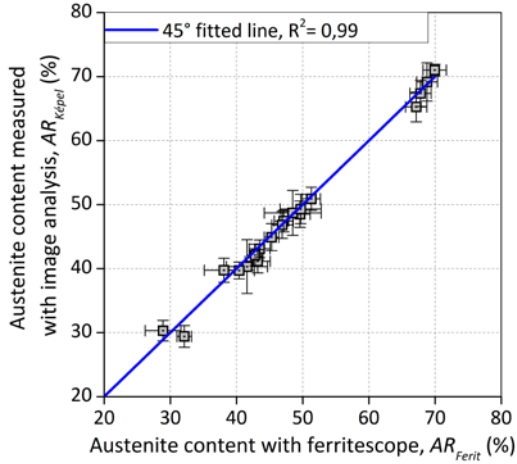

Figure 1. The results of austenite content measured with image analysis, after optimal ethcing cycle ($AR_{Képel}$), compared to the austenite contents measured by ferritescope (AR_{Ferit}).

In order to evaluate the validation process of the etching cycles, I introduced a unitless number DoU (degree of usability), which is specific to the result of a ferritoscopic measurement and shows an exponential relationship with the contrast value (ΔG) between the two phases (see Figure 2).

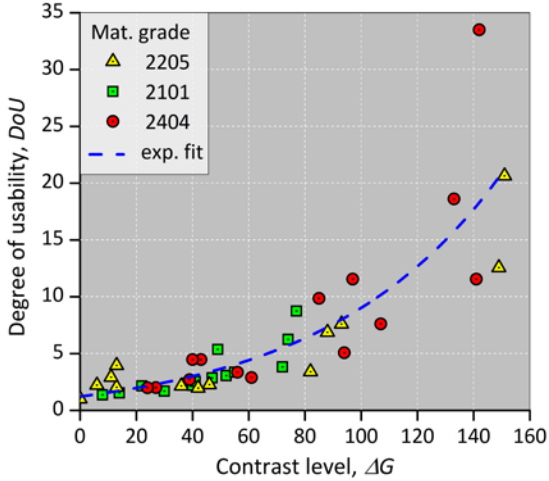

Figure 2. The DoU (degree of usability) number as a function of ΔG contrast levels, using Beraha-II type etchant.

Summarizing the results of the validation, I concluded that the highest contrast contrast resulting etching cycle can be considered as optimal for the determination of austenite content with the image analysis software. Based on these results, I have written my 1st thesis.

Investigation of the heat affected zone

For the investigation of the austenite and nitrogen content of the heat affected zone, I used Gleeble thermomechanical simulator (for grade 2205, see Figure 3) and TIG-welding (for all three examined material grades). With the Gleeble thermomechanical simulator it is possible to study wider heat input ranges than TIG-welding and the heat input can be programmed.

During the Gleeble simulation, the specimens were heated to a peak temperature of 1350 °C (purely ferritic range) under 10 s, where they were kept in argon shielding for 1 s. In order to investigate the different critical cooling times between 1200 and 800 °C ($\Delta t_{12/8}$), the samples were cooled with water or blown air after the heating cycle.

In the case of the autogenous TIG-welding without consumables, the $\Delta t_{12/8}$ was measured with thermocouples and a thermal imaging camera.

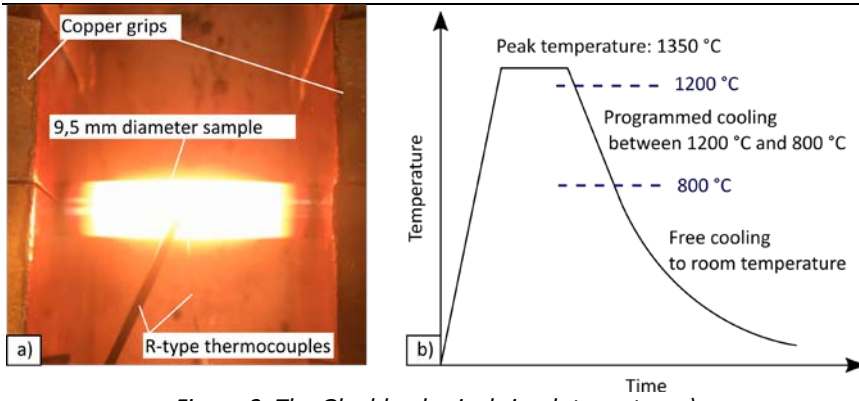

Figure 3. The Gleeble physical simulator setup a) and the schematic representation of the applied thermal cycle b).

As a result, I have found that the $\Delta t_{12/8}$ cooling time (related to the heat input) has the greatest effect on the austenite content of the heat affected zone (see Figure 4). The total dissolved nitrogen content does not change significantly during solid state reheating. For the estimation of the austenite content of the heat affected zone, I have determined the constants of the Johnson–Mehl–Avrami–Kolmogorov equation for a non-isothermal state, which can be used to calculate the austenite content of the heat effect zone for 2205 materials.

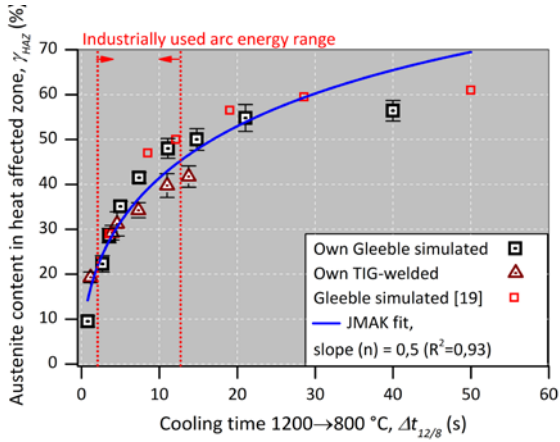

Figure 4. The fitted JMAK equation for the determination of the austenite content of the heat affected zone beased on own and ref. [19] *results for duplex stainless steel grade 2205.*

Based on these results I have written my 2nd and 3rd thesis.

Investigation of the weld metal in case of TIG welding with argon + nitrogen shielding gas

For the investigation of the austenite and nitrogen content of the weld metal, autogenous TIG-welding with two different arc energies (0.53 and 0.68 kJ/mm) and argon + 0-50 % nitrogen gas shielding were appliead for all the investigated three material grades.

In order to calculate the dissolved nitrogen content in the weld metal, I created an improved model, based on previous models, which schematic illustration is shown in Figure 5.

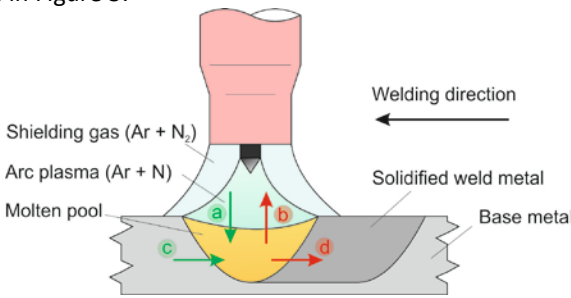

Figure 5. Schematic illustration of the nitrogen absorption: (a,c), and desorption: (b,d) during autogenous tungsten inert gas (TIG) welding of DSS.

The improved model gives the expected nitrogen content of the weld metal with a smaller difference (<10 %) than previous models. A comparison of the existing models for one case (2205 material grade and 0.68 kJ/mm arc energy) is shown in Figure 6.

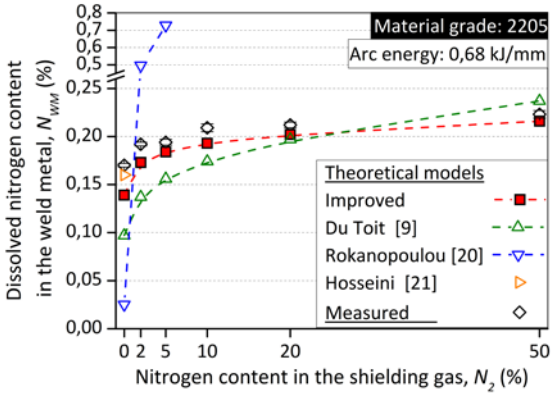

Figure 6. The comparison of my improved model and the previous models [9, 20, 21] *for the calculation of weld metal nitrogen content.*

I have supplemented the improved model with an own parameter, which takes the initial nitrogen and chromium content of the base material into attention. The parameter-supplemented model gives the expected nitrogen content of the weld metal with less then 5 % difference (for all the investigated cases) for autogenous TIG-welding using argon + nitrogen shielding gas (see Figure 7. for material grade 2205)

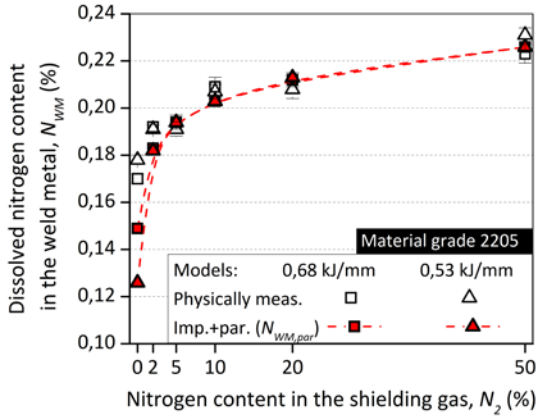

Figure 7. The weld metal nitrogen contents calculated by the parameter-supplemented and improved model ($N_{WM,par}$), compared to the measured (N_{WM}) values.

Based on these results I have written my 4th and 5th thesis.

Investigation of the weld metal in case of TIG welding with argon shielding gas

The improved model supplemented with an own parameter gives an adequate calculation for the nitrogen shielding gases. Therefore, for a wider arc energy range (0.25-2.95 kJ/mm), the extent of nitrogen reduction in the weld metal was investigated in the case of autogenous TIG welding with using argon shielding gas. I have determined the parameters of an equation which, given the nitrogen content of the base material and the solidification time, gives the percentage reduction in the nitrogen content of the weld metal compared to the nitrogen content of the base material. The defined equation gives a better approximation than the previous models and can be applied to a variety of duplex stainless steel grades (see Figure 8).

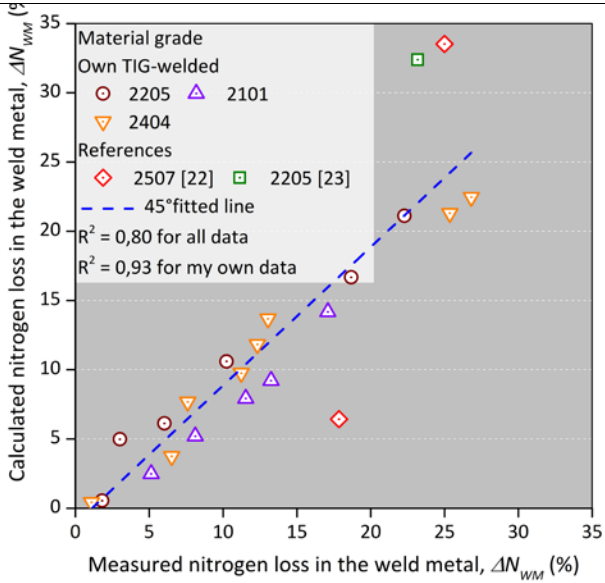

Figure 8. Comparison of the relative reduction in nitrogen content of the welded metal, calculated according to the defined equation, supplemented with literature data [22, 23].

In addition, I also defined that, contrary to the change in the austenite content of the heat affected zone, the increasing arc energy values in the weld metal result in a decrease in the austenite content (see Fig. 9 for 2205 base material). The main reason for this is the decrease in dissolved nitrogen content of the weld metal with increasing arc energy. Based on these results I have written my 6th and 7th thesis.

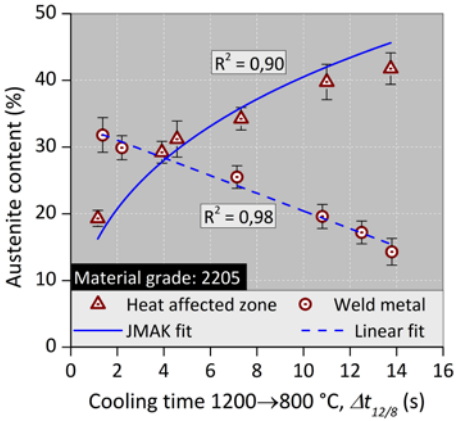

Figure 9. The change of the austenite content in the heat affected zone and in the weld metal as a function of the $\Delta t_{12/8}$ cooling time for 2205 grade. For the other material grades the relationships can be found in the dissertation.

THESES

THESIS 1

I have developed a new etching method for the determination of austenite content by image analysis software on the metallographic specimens of gas tungsten arc welded welds of duplex stainless steels. When using Beraha-II etching agent (85 mL H_2O + 15 mL HCl + 1 g $K_2S_2O_5$), the following etching cycles provide the highest contrast between the delta ferrite and austenite phases:

- 2 x 12 s for steel X2CrNiMoN22-5-3 (1.4462),
- 1 × 24 s for steel X2CrMnNiN21-5-1 (1.4162),
- 2 × 6 s for X2CrNiMnMoCuN24-4-3-2 (1.4662) duplex stainless steel grades.

In the case of multiple etching, the two etching steps must be performed sequentially immediately after each other, with ethanol washing in-between the etching steps.

The results of image analysis software, obtained with the highest contrast were validated by magnetic measurement based ferritescope measurement, manual point count method according to ASTM E562-11 and electron backscatter diffraction (EBSD) measurement.

Based on the results of the validation, the highest contrast etching cycle is considered to be optimal for the determination of austenite content by image analysis software.

Related publications:
[S1] [S2] [S3] [S4] [S5] [S6]

THESIS 2

When welding of duplex steel X2CrNiMoN22-5-3 (1.4462), the measured nitrogen content in the heat zone does not change substantially, the critical $\Delta t_{12/8}$ cooling time having the greatest effect on the austenitic content of the heat affected zone.

Related publications:
[S1] [S6]

THESIS 3

For the welding of X2CrNiMoN22-5-3 (1.4462) duplex stainles steel, the following Johnson-Mehl-Avrami-Kolmogorov equation, written for a non-isothermal state, can be used to estimate the austenitic content (γ_{HAZ} *(%)*) in the heat affected zone:

$$\gamma_{HAZ} = 100 \cdot (1 - \exp(k \cdot (\Delta t_{12/8})^n))\,(\%)$$

where the process rate constant is k = -0.17 and the Avrami exponent n = 0.5.

Related publications:
[S1] [S6]

THESIS 4

I have developed a model (based on equations 6.1 to 6.27) that gives a better accuracy of the expected nitro-gen content (NWM) of the weld metal than previous mo-dels. The model is valid for duplex steel grades X2CrNiMoN22-5-3 (1.4462), X2CrMnNiN21-5-1 (1.4162) and X2CrNiMnMoCuN24-4-3-2 (1.4662), in case of autogenous gas tungsten arc welding, using argon + 0-50 % nitrogen shileding gas, in the 0.53 and 0.68 kJ/mm arc energy range.

The model can be found in the dissertation on the pages of 42.-47., with the same numebring system.

Equation	Unit	Numbering in the dissertation
$N(g) \rightarrow \underline{N}$	-	6.1
$\frac{d\underline{N}}{dt} = \frac{100AK_a}{\rho V}\left[N(g) - \frac{N_{WM}}{K}\right]$	-	6.2
$V = \frac{\pi}{6}h\left(3\left(\frac{L}{2}\right)^2 + h^2\right)$	m^3	6.3
$K_a = 3{,}5 \cdot 10^4$	$kg/(m^2 \cdot s \cdot atm)$	6.4
$\rho = 1000 \cdot \left(-7{,}2 \cdot 10^{-4}(T - T_m) + 7{,}04\right)$	kg/m^3	6.5
$T = 1995$	K	6.6
$T_m = 1733$	K	6.7
$N(g) = \sqrt{P_{N2}}\,\exp\left(-\frac{\Delta G^\circ{}_1}{RT_d}\right)$	atm	6.8
$P_{N2} = \frac{N_2}{100}$	atm	6.9

Equation	Unit	Numbering in the dissertation
$\frac{1}{2}N_2 \rightarrow N(g)$	-	6.10
$\Delta G^\circ_1 = 362560 - 65{,}56T_d$	J/mol	6.11
$T_d = 1995$	K	6.12
$R = 8{,}314$	J/(mol·K)	6.13
$K = \frac{\sqrt{K'}}{K_1}$	K	6.14
$K' = \frac{(N_{eq})^2}{P_{N2}}$	kg/(m²·s·atm)	6.15
$\log(\underline{N}_{eq}) = -\frac{247}{T} - 1{,}22 - \left(\frac{4780}{T} - 1{,}51\right)\log f_{N,T} - \left(\frac{1760}{T} - 0{,}91\right)(\log f_{N,T})^2$	-	6.16
$\log f_{N,T} = \left(\frac{2538}{T} - 0{,}355\right)\cdot \log f_{N,1873}$	-	6.17
$\log f_{N,1873} = e_N{}^N \%N + e_N{}^{Mn} \%Mn + e_N{}^{Si} \%Si + e_N{}^P \%P + e_N{}^{Cr} \%Cr + e_N{}^{Mo} \%Mo + e_N{}^{Ni} \%Ni + \left(\gamma_N{}^{Cr} \%Cr^2 + \gamma_N{}^{Mn} \%Mn^2 + \gamma_N{}^{Mo} \%Mo^2 + \gamma_N{}^{Ni} \%Ni^2\right)$	-	6.18
$K_1 = \frac{N(g)}{\sqrt{P_{N2}}}$	atm²	6.19
$2\underline{N} \rightarrow N_2$	-	6.20
$\frac{d\underline{N}}{dt} = \frac{100AK_d}{\rho V}\left(N_{WM}{}^2 - N_{eq.steel}{}^2\right)$	-	6.21
$K_d = \frac{10^{(-6340/T + 1.85)}}{1 + 130 f_S S}$	kg/(m² · s)	6.22
$\log f_S = Cr\left(-\frac{94{,}2}{T} + 0{,}040\right)$	-	6.23
$N_{eq.steel} = \frac{\sqrt{P_{N2}} \cdot \exp\left(-\frac{\Delta G^\circ_2}{RT}\right)}{f_{N,T}}$	%	6.24
$\Delta G^\circ_2 = 3598{,}2 + 23{,}89 \cdot T$	J/mol	6.25
$\frac{d\underline{N}}{dt} = N \cdot \left(\frac{v}{L}\right)$	-	6.26
$\frac{d\underline{N}}{dt} = -N_{WM}\left(\frac{v}{L}\right)$	-	6.27

Related publications:
[S1] [S4] [S7] [S8]

THESIS 5

I introduced a parameter based on the initial nitrogen and chromium content of the base material ($N_{WM,par}$), by which the model developed to predict the expected nitrogen content of the weld metal (NWM, Thesis 4) gives the weld metal nitrogen content with less than 5 % error, compared to the actual measured nitrogen content.

The parameter I introduced: $N_{WM,par} = N_{WM} + \left(\frac{N}{10} + \frac{Cr - 22}{50} \right)$ (%)

where N_{WM} is the nitrogen content of the weld metal according to the newly developed model (Thesis 4), N and Cr are the initial nitrogen and chromium contents of the base material, respectively. All quantities are interpreted as percentages. The model with the $N_{WM,par}$ parameter is valid for duplex steel grades X2CrNiMoN22-5-3 (1.4462), X2CrMnNiN21-5-1 (1.4162) and X2CrNiMnMoCuN24-4-3-2 (1.4662), in case of autogenous gas tungsten arc welding, using argon + 0-50% nitrogen shileding gas, in the 0.53 and 0.68 kJ/mm arc energy range.

Related publications:
[S8] [S9]

THESIS 6

I determined the parameters of an equation, which is dependent on the base materials initial nitrogen content (N) and gives the expected loss of nitrogen in the weld metal (ΔN_{WM}), as a function of the solidification time (S_t), for duplex stainless steel grades X2CrNiMoN22-5-3 (1.4462), X2CrMnNiN21-5-1 (1.4162) and X2CrNiMnMoCuN24-4-3-2 (1.4662), in case of autogenous gas tungsten arc welding, using argon shielding gas. The parameters of the equation are:

$$\Delta N_{WM} = 17{,}4 - 113{,}1 \cdot N - 23{,}4 + 168{,}5 \cdot N \cdot S_t \ (\%)$$

where S_t is the solidification time in seconds and N is the base materials initial nitrogen content in percentages.

Related publications:
[S1] [S6]

THESIS 7

In case of autogenous gas tungsten arc welding of duplex stainless steel grades X2CrNiMo22-5-3 (1.4462), X2CrMnNiN21-5-1 (1.4162) and X2CrNiMnMoCuN24-4-3-2 (1.4662), using argon shielding gas, the increasing arc energy causes the austenite content of the weld metal to decrease, mainly due to the decreasing nitrogen content in the weld metal with the increasing arc energy, on the contrary to the increasing austenite content in the heat affected zone with the increasing arc energy.

Related publications:
[S1] [S6]

PUBLICATIONS RELATED TO THE THESES

Journal papers

[S1] Varbai B, Adonyi Y, Baumer R, Pickle T, Dobránszky J, Májlinger K. Weldability of Duplex Stainless Steels - Thermal Cycle and Nitrogen Effects. *Welding Journal.* 2019;98(3):78–87. DOI:10.29391/2019.98.006, **WoS IF: 1,652, Q3**

[S2] Varbai B, Pickle T, Májlinger K. Development and Comparison of Quantitative Phase Analysis for Duplex Stainless Steel Weld. *Periodica Polytechnica Mechanical Engineering.* 2018;62(3):247–253. 2018. DOI:10.3311/PPme.12234

[S3] Varbai B, Mészáros I, Májlinger K. Effects of different backing gases on 2404 duplex stainless steel welds. *IOP Conference Series: Materials Science and Engineering*, 2018;426(1):012051. DOI:10.1088/1757-899X/426/1/012051

[S4] Varbai B, Májlinger K. Physical and Theoretical Modeling of the Nitrogen Content of Duplex Stainless Steel Weld Metal: Shielding Gas Composition and Heat Input Effects. *Metals*. 2019;9(7):762. DOI:10.3390/met9070762, **WoS IF: 2,259, Q1**

[S5] Varbai B, Májlinger K. Optimal etching sequence for austenite to ferrite ratio evaluation of two lean duplex stainless steel weldments. *Measurement.* 2019;147:106832. DOI:10.1016/j.measurement.2019.07.060, **WoS IF: 2,791, Q2**

[S6] Varbai B, Pickle T, Májlinger K. Effect of heat input and role of nitrogen on the phase evolution of 2205 duplex stainless steel weldment. *International Journal of Pressure Vessels and Piping.* 2019;176: 103952. DOI:10.1016/j.ijpvp.2019.103952, **WoS IF: 2,075, Q2**

[S8] Varbai B, Májlinger K. A nitrogén szerepe a duplex acélok ívhegesztésekor. *Hegesztéstechnika.* 2019;30(3):63–67.

Conference papers

[S7] Varbai B, Lados L, Májlinger K. A védőgázhoz kevert nitrogén hatása duplex korrózióálló acélok volfrámelektródás védőgázos ívhegesztésekor. In I. Barabás (Ed.), *XXVII. Nemzetközi Gépészeti Konferencia OGÉT 2019* (pp. 597–600). Nagyvárad, Románia: Erdélyi Magyar Tudományos Társaság. 2019.

Oral presentation with no paper yet

[S9] Varbai B, Májlinger K. Determining the effect of nitrogen addition to the shielding gas for duplex stainless steel welds microstructure. Szóbeli előadás. *72nd International Institute of Welding Annual Assembly and International Conference*. Pozsony. 2019.07.12.

REFERENCES

[1] International Stainless Steel Forum. Stainless Steel in Figures 2018. Shanghai; 2018.

[2] Chater J. The year in stainless steel: industry sees growth, but over-production still an issue. *Stainless Steel World*. 2019;31:28–31.

[3] Yoshida T. Duplex Steel Market in Asia and NSSC ' s Solution. *8th Duplex Stainless Steel Conference*. Beaune, France; 2010.

[4] Boillot P, Peultier J. Use of stainless steels in the industry: recent and future developments. *Procedia Engineering*. 2014;83:309–321.

[5] Liljas M. 80 Years With Duplex Steels, a Historic Review and Prospects for the Future. *6th European Stainless Steel Conference*. Helsinki, Finland: Jernkontoret; 2008.

[6] Haldorsen LM. Welding duplex - challenges faced and experience gained. *Stainless Steel World*. 2016;53–58.

[7] Gunn RN. Duplex stainless steels : microstructure, properties and applications. Abington: Abington Publishing; 1997.

[8] Gutierrez I, Iza-Mendia A, Charles J, et al. Duplex stainless steels. 1st ed. In: Alvarez-Armas I, Degallaix-Moreuil S, editors. 1st ed. London, Hoboken: ISTE Ltd and John Wiley & Sons, Inc.; 2009.

[9] du Toit M. The Behaviour of Nitrogen during the Autogenous Arc Welding of Stainless Steel. University of Pretoria. 2001. *PhD dissertation*.

[10] Fábián ER. Duplex acélok lézersugaras hegesztésekor bekövetkező szövetszerkezet-változások elemzése. Budapesti Műszaki és Gazdaságtudományi Egyetem. 2014. *Welding engineer thesis*.

[11] Quiroz V, Gumenyuk A, Rethmeier M. Laser Beam Weldability of High-Manganese Austenitic and Duplex Stainless Steel Sheets. *Welding in the World*. 2012;56:9–20.

[12] Başyiğit A, Kurt A. The Effects of Nitrogen Gas on Microstructural and Mechanical Properties of TIG Welded S32205 Duplex Stainless Steel. *Metals*. 2018;8:226.

[13] Sales AM, Westin EM, Jarvis BL. Effect of nitrogen in shielding gas of keyhole GTAW on properties of duplex and superduplex welds. *Welding in the World*. 2017;61:1133–1140.

[14] Pamuk S, Sojiphan K. Effects of argon-nitrogen backing gas ratios on microstructure and corrosion resistance of duplex stainless steel pipe ASTM A790 welds by gas tungsten arc welding process. *Materials Today: Proceedings*. 2018;5:9512–9518.

[15] Igual Muñoz A, García Antón J, Guiñón JL, et al. Effect of nitrogen in Argon as a shielding gas on tungsten inert gas welds of duplex stainless steels. *Corrosion*. 2005;61:693–705.

[16] Migiakis K, Papadimitriou GD. Effect of nitrogen and nickel on the microstructure and mechanical properties of plasma welded UNS S32760 super-duplex stainless steels. *Journal of Materials Science*. 2009;44:6372–6383.

[17] Reyes-Hernández D, Manzano-Ramírez A, Encinas A, et al. Addition of nitrogen to GTAW welding duplex steel 2205 and its effect on fatigue strength and corrosion. *Fuel*. 2017;198:165–169.

[18] Bhatt RBB, Kamat HSS, Ghosal SKK, et al. Influence of Nitrogen in the Shielding Gas on Corrosion Resistance of Duplex Stainless Steel Welds. *Journal of Materials Engineering and Performance*. 1999;8:591–597.

[19] Mei He BS. Evaluation of the Susceptibility of Duplex Stainless Steel 2205 to Hydrogen Assisted Cracking in REAC Systems. 2016. The Ohio State University. *MSc thesis*.

[20] Rokanopoulou A, Skarvelis P, Papadimitriou GD. Welding design methodology for optimization of phase balance in duplex stainless steels during autogenous arc welding under Ar–N2 atmosphere. *Welding in the World*. 2019;63:3–10.

[21] Hosseini VA, Wessman S, Hurtig K, et al. Nitrogen loss and effects on microstructure in multipass TIG welding of a super duplex stainless steel. *Materials and Design*. 2016;98:88–97.

[22] Hosseini VA. Influence of multiple welding cycles on microstructure and corrosion resistance of a super duplex stainless steel. 2016. Högskolan Väst. *Licentitate thesis*.

[23] Hertzman S, Pettersson RJ, Blom R, et al. Influence of shielding gas composition and welding parameters on the N-content and corrosion properties of welds in N-alloyed stainless steel grades. *ISIJ International*. 1996;36:968–976.